Philosophical Magazine A

Atomistic simulation of titanium. I. A bond-order potential

A. Girshick [a] , A. M. Bratkovsky [b] , D. G. Pettifor [b] & V. Vitek [a]

[a] Department of Materials Science and Engineering,
University of Pennsylvania, Philadelphia, Pennsylvania,
19104-6272, USA

[b] Department of Materials, University of Oxford, Parks Road,
Oxford, OX1 3PH, England
Version of record first published: 12 Aug 2009.

PLEASE SCROLL DOWN FOR ARTICLE

Atomistic simulation of titanium
I. A bond-order potential

By A. GIRSHICK†, A. M. BRATKOVSKY‡, D. G. PETTIFOR‡
and V. VITEK†

† Department of Materials Science and Engineering, University of Pennsylvania,
Philadelphia, Pennsylvania, 19104-6272, USA
‡ Department of Materials, University of Oxford, Parks Road, Oxford OX1 3PH,
England

ABSTRACT

The bond-order potential for hcp Ti has been constructed in the framework of a tight-binding description of the binding energy. In this scheme the energy consists of two parts: the bond part that comprises the d-electron contribution to bonding, and a pairwise part. Both parts contain fitting parameters but are treated independently. The bond part reproduces the most important characteristics of the d-band and Cauchy pressures, and the pairwise part complements the bond part so as to reproduce exactly the equilibrium lattice parameters and to a good approximation the elastic moduli. The potential is tested by examining the mechanical stability of the hcp lattice with respect to a variety of large deformations. It is applied to a study of dislocation behaviour in Ti in the accompanying paper, part II.

§1. INTRODUCTION

Atomistic calculations of extended crystal defects, such as dislocations and interfaces, have now become a common tool for investigation of their structure and properties (see, for example, volumes edited by Tersoff et al. (1989), Mark et al. (1992), Broughton et al. (1993), Gonis et al. (1996) and Voter (1996)). The essential precursor of such studies is a description of atomic interactions or, more generally, knowledge of the dependence of the total energy of the system on the positions of the atoms. In principle, this is available in ab initio total energy calculations based on the local density approximation to the density functional theory (for example Pettifor and Cottrell (1992)). However, such calculations are ordinarily only feasible when the number of atoms included in the calculation is well below 100 and this is usually totally inadequate for extended defects. Hence, the bulk of the dislocation and interfacial modelling has been made using much simpler approaches.

In recent years, the most successful in studies of metallic materials were the embedded-atom method (EAM) (Daw and Baskes 1984, Daw et al. 1993) and many-body potentials of the Finnis–Sinclair (1984) type. These empirical schemes are central-force descriptions of atomic interactions, that is the total energy is only a function of separations of atomic pairs and any possible directional character of bonding is excluded but, contrary to the pair-potentials (for example Vitek (1996)), the cohesive part of the total energy has a many-body character (for example Ackland et al. (1988) and Foiles (1996)). This approach was employed very successfully in many studies involving noble metals and their alloys (for example Ackland

et al. (1987) and Daw *et al.* (1993)), as well as nickel and Ni–Al alloys (Voter and Chen 1987; Ludwig and Gumbsch 1995, Yan *et al.* 1996). This approach was also applied to bcc transition metals (Ackland and Thetford 1987) and Ti (Ackland 1992) but its success was limited since the angular component of the bonding in these metals is significant. For example, it is shown in the accompanying paper, part II (Girshick *et al.* 1998), that for Ti incorrect slip planes are predicted in this scheme. In addition, it is well known that in transition metals the relative stability of alternate crystal structures is controlled by the level of the filling of the d band (Pettifor 1983; 1995) and the bonding mediated by the d electrons has a covalent character. Consequently, it can be expected that the covalent component of bonding may also play a significant role in determination of low-energy structures of extended lattice defects in transition metals and a description of atomic interactions that includes such character of bonding is needed for reliable atomistic studies (Carlsson 1991, Foiles 1993, Moriarty 1994, Pettifor *et al.* 1995, Xu and Moriarty 1996).

The semiempirical method in which the required covalent character of bonding is included is the tight-binding method that comprises the two-centre d–d hopping integrals. In recent years this method has been reformulated in terms of bond order potentials (Pettifor 1989, Aoki 1993, Aoki and Pettifor 1994, Horsfield *et al.* 1996a, b). The primary advantage of this semiempirical treatment is that all the calculations are done in the real space and forces on atoms arising from the bond energy that comprises the d-electron contribution, can be evaluated following the Hellmann (1937)–Feynman (1939) theorem. Also, bond-order potentials belong to the class of order-N methods (Bowler *et al.* 1997) and can therefore be used in calculations involving a large number of particles which is needed in studies of extended defects.

In this paper we first summarize the principal features of the tight-binding method with two-centre matrix elements in which the energy is divided into the bond part that describes the covalent type bonding and the pairwise part. This approach serves as a basis for definition of bond-order potentials. The formalism of the bond-order potentials is then described in detail together with the steps involved in their construction which includes fitting of a number of equilibrium electronic, structural and mechanical properties. The construction of the bond-order potential for hcp Ti is then presented and its applicability to studies of defective structures tested. This is done by investigating the stability of the hcp structure with respect to large homogeneous deformations and alternative structures with similar packing. In part II, in the context of studies of stacking-fault-type defects, we also test the mechanical stability with respect to large shears parallel to basal and prism planes and use the potential in atomistic studies of dislocations in Ti.

§ 2. ENERGY AND FORCES WITHIN THE TIGHT-BINDING METHOD

The trends in experimental cohesive energies and ground-state structures within the non-magnetic transition-metal series have been shown to be determined by the bonding behaviour of the valence d electrons (Friedel 1969; Pettifor 1983, 1995). Therefore, in the tight-binding scheme, the energy of a system of atoms of a transition metal (Ti) can be divided into two parts: firstly the bond energy arising from formation of the valence d band that comprises terms dependent on bond angles, and secondly the pairwise part of the energy representing to a good approximation the overlap repulsion and electrostatic interaction between the atoms (Sutton *et al.*1988, Pettifor *et al.* 1989, Skinner and Pettifor 1991). The binding energy also

includes an attractive contribution of about 2 eV per atom that arises from hybridization between the nearly free-electron s–p band and the tight-binding d band (Gelatt *et al.* 1977). Although we do not expect this hybridization term to be strictly pairwise in character, we did not find any need during the fitting procedure to describe this term in a more complex manner, and so we have included this attractive contribution implicitly in the pairwise part of the energy.

In order to damp down the long-range Friedel oscillations that are present in metals a fictitious finite temperature of the electrons needs to be introduced in order to achieve rapid real-space convergence of the bond-order potentials (for example Bowler *et al.* (1997) figure 2 (*b*)). For this reason we work with the free energy $\mathcal{F}$ rather than the internal energy U. In the tight-binding framework the free energy of a system of N atoms situated at rest at positions $\mathbf{R}_k$ ($k = 1, \ldots, N$) with their valence electrons held at temperature T_e is

$$\mathcal{F} = \frac{1}{2} \sum_{i \neq j} V(R_{ij}) + \mathcal{F}_B. \tag{1}$$

The first term is the pairwise part of the energy, defined by the pair potential $V(R_{ij})$, describing the interaction between atoms i and j separated by the distance R_{ij}. The pair potential is repulsive at small separations of the atoms but may be attractive at larger separations owing to electrostatic and hybridization contributions. The second term, the bond part, is the free energy of the valence d electrons at the effective electronic temperature T_e and it can be written as (Mermin 1965)

$$\mathcal{F}_B = \sum_i (U_i - T_e S_i), \tag{2}$$

where the internal energy U_i is the d bond energy and S_i the electronic entropy associated with atom i.

The internal energy is given by

$$U_i = 2 \sum_\alpha \int \varepsilon n_{i\alpha}(\varepsilon) f\left(\frac{\varepsilon - \mu}{k_B T_e}\right) d\varepsilon, \tag{3}$$

where $n_{i\alpha}(\varepsilon)$ is the local density of states associated with orbital α on an atom i (with $\alpha = xy$, yz, xz, $x^2 - y^2$ and $3z^2 - r^2$), the pre-factor 2 accounts for the spin degeneracy in non-magnetic systems, $f(x) = 1/(1 + \exp x)$ is the Fermi–Dirac function, μ is the chemical potential determined by the number of valence electrons and the electronic temperature T_e, and k_B is the Boltzmann constant. The local density of states is calculated within the two-centre orthogonal tight-binding approximation and may be expressed in terms of the diagonal matrix elements of the Green's function, namely

$$n_{i\alpha}(\varepsilon) = -\frac{1}{\pi} \lim_{\eta \to 0} \{ \mathrm{Im} \, [G_{i\alpha,i\alpha}(\varepsilon + \mathrm{i}\eta)] \}, \tag{4}$$

where η is an infinitesimally small positive number. The electronic entropy is given by

$$S_i = 2 \sum_\alpha \int n_{i\alpha}(\varepsilon) \sigma\left(\frac{\varepsilon - \mu}{k_B T_e}\right) d\varepsilon, \tag{5}$$

where $\sigma(x)$ is the entropic density given by

$$\sigma(x) = -k_B \{ f(x) \log [f(x)] + [1 - f(x)] \log [1 - f(x)] \}. \tag{6}$$

It is important to note that the energy ε is measured with respect to the on-site atomic energy level E_i so that $\varepsilon = E - E_i$. Thus bonding states with $E < E_i$ give a negative contribution to the d bond energy (equation (3)) whereas antibonding states with $E > E_i$ give a positive contribution. There is no ionic contribution present in equation (1) because the on-site energies E_i are adjusted self-consistently to maintain local charge neutrality (LCN) with respect to each atom (see §3). This reflects the perfect screening properties of metals (Pettifor 1995).

The bond energy U_i associated with atom i may be decomposed explicitly in terms of the contributions from individual bonds which atom i makes with the neighbouring atoms j. Using the defining equation for the Green's function (for example Horsfield *et al.* (1996a, b)), we have

$$U_i = \frac{1}{2} \sum_{j \neq i} \sum_{\alpha, 3} 2 \langle i\alpha | \hat{H} | j\beta \rangle \Theta_{j3, i\alpha}, \tag{7}$$

where $\langle i\alpha | \hat{H} | j\beta \rangle$ is the Hamiltonian matrix element between the orbital α on site i and the orbital β on site j. Within the two-centre approximation these matrix elements are determined solely by the fundamental bond integrals $dd\sigma(R_{ij})$, $dd\pi(R_{ij})$ and $dd\delta(R_{ij})$ and the direction cosines defining the bond direction $\mathbf{R}_{ij}$ (Slater and Koster 1954). The matrix elements $\Theta_{j3, i\alpha}$ are given by

$$\Theta_{j3, i\alpha} = -\frac{2}{\pi} \lim_{\eta \to 0} \left[\int \{ \operatorname{Im} [G_{i\alpha, j3}(\varepsilon + i\eta)] \} f\left(\frac{\varepsilon - \mu}{k_B T_e} \right) d\varepsilon \right]. \tag{8}$$

For a given pair of neighbouring atoms i and j, $\Theta_{j3, i\alpha}$ defines the appropriate *bond order* matrix. This can be seen by rewriting equation (8) in terms of the diagonal matrix elements of the Green function with respect to the bonding states $|+\rangle = (|i\alpha\rangle + |j\beta\rangle)/2^{1/2}$ and antibonding states $|-\rangle = (|i\alpha\rangle - |j\beta\rangle)/2^{1/2}$ so that

$$\Theta_{j3, i\alpha} = -\frac{1}{\pi} \lim_{\eta \to 0} \left[\int \{ \operatorname{Im} [G_{++}(\varepsilon + i\eta) - G_{--}(\varepsilon + i\eta)] \} f\left(\frac{\varepsilon - \mu}{k_B T_e} \right) d\varepsilon \right]. \tag{9}$$

It then follows from equation (4) that

$$\Theta_{j3, i\alpha} = N_+ - N_-, \tag{10}$$

where N_+ and N_- are the number of electrons with a given spin associated with the bonding and antibonding states respectively. Thus, for any given pair of neighbouring transition-metal atoms i and j, we are able to quantify the bond order of the resultant $dd\sigma$, $dd\pi$ and $dd\delta$ bonds (for example Sutton *et al.* (1988)).

Atomistic simulations require the calculation not only of the energy but also of the forces acting on individual atoms. It follows from equations (1), (2), (5) and (7) that the force acting on atom k is

$$\mathbf{\Phi}_k = -\operatorname{grad}_{R_k} \mathbf{F} = -\frac{1}{2} \sum_{i \neq j} \operatorname{grad}_{R_k} V - \sum_{i \neq j} \sum_{\alpha, 3} \operatorname{grad}_{R_k} (\langle i\alpha | \hat{H} | j\beta \rangle) \Theta_{j3, i\alpha}, \tag{11}$$

since the theorem of Hellmann (1937) and Feynman (1939) guarantees that the first-order change in the entropic contribution $-T_e \delta S$ exactly cancels the first-order change in the bond-order contribution $H \delta \Theta$. The calculation of the derivative of the pair potential and the Hamiltonian matrix elements is straightforward. Thus, provided that the bond order $\Theta_{j3, i\alpha}$ is computed sufficiently accurately for the Hellmann-Feynman theorem to apply, we may write down directly not only the bond energy (equation (7)) but also the forces (equation (11)).

§3. BOND-ORDER POTENTIAL FORMALISM

It follows from equation (3) that the bond energy associated with atom i can be written as

$$U_i = 10 \int \varepsilon n_i(\varepsilon) f\left(\frac{\varepsilon - \mu}{k_B T_e}\right) d\varepsilon, \tag{12}$$

where $n_i(\varepsilon)$ is the average density of states per orbital per spin, namely

$$n_i(\varepsilon) = \tfrac{1}{5} \sum_\alpha n_{i\alpha}(\varepsilon). \tag{13}$$

We expect $n_i(\varepsilon)$ to be determined primarily by the *local* environment of atom i rather than by the overall *global* nature of the solid. This can be expressed mathematically using the recursion method (Haydock 1980) to write the diagonal element of the Green function (cf equation (4)) as the continued fraction

$$G_{ii}(z) = \cfrac{1}{z - a_0^i - \cfrac{(b_1^i)^2}{z - a_1^i - \cfrac{(b_2^i)^2}{z - \dots}}}, \tag{14}$$

where the recursion coefficients $\{a_n^i, b_n^i\}$ are determined by the Lanczos (1950) algorithm.

The recursion coefficients may be expressed in terms of the moments of the density of states.

$$\mu_p^i = \int \varepsilon^p n_i(\varepsilon) \, d\varepsilon. \tag{15}$$

In particular, the first two recursion coefficients are given by

$$a_0^i = \mu_1^i \tag{16a}$$

and

$$(b_1^i)^2 = \mu_2^i - (\mu_1^i)^2. \tag{16b}$$

Therefore a_0^i locates the centre of gravity of the density of states whereas b_1^i gives its rms width. It may be shown (for example Pettifor (1995)) that a_1^i is a measure of the skewness of the band, whereas b_2^i is a measure of the unimodal versus bimodal behaviour. Moreover, the dependence of the recursion coefficients on the local environment has been demonstrated explicitly since the pth moment can be written as the following sum over all paths of length p that start and finish at the given atom i:

$$\mu_p^{(i)} = \tfrac{1}{5} \sum_{j_1, j_2, \dots, j_{p-1}} \sum_{\alpha, \alpha_1, \alpha_2, \dots, \alpha_{p-1}} \langle i\alpha | \hat{H} | j_1 \alpha_1 \rangle \langle j_1 \alpha_1 | \hat{H} | j_2 \alpha_2 \rangle$$
$$\cdots \langle j_{p-2} \alpha_{p-2} | \hat{H} | j_{p-1} \alpha_{p-1} \rangle \langle j_{p-1} \alpha_{p-1} | \hat{H} | i\alpha \rangle. \tag{17}$$

This expression follows because

$$\mu_p^i = \tfrac{1}{5} \sum_\alpha \int \varepsilon^p n_{i\alpha}(\varepsilon) \, d\varepsilon = \tfrac{1}{5} \sum_\alpha \langle i\alpha | \hat{H}^p | i\alpha \rangle. \tag{18}$$

In practice just the first few recursion coefficients in the continued fraction are calculated exactly. The remainder are approximated by the constant values a_∞ and b_∞ (Beer and Pettifor 1984).

The bond order $\Theta_{j\beta,i\alpha}$ is also dependent on the sets of recursion coefficients $\{a_n^i, b_n^i\}$ and $\{a_n^j, b_n^j\}$ associated with atoms i and j respectively. It takes the form (see Horsfield *et al.* (1996a) and references therein)

$$\Theta_{j\beta,i\alpha} = -\sum_{k=j,i} \sum_{m=0}^{\infty} \chi_{0m,m0}^k (N_d, T_e, \{a_n^k, b_n^k\})(\delta a_m^k)_{j\beta,i\alpha}$$

$$- \sum_{k=j,i} \sum_{m=1}^{\infty} \chi_{0(m-1),m0}^k (N_d, T_e, \{a_n^k, b_n^k\})(2\,\delta b_m^k)_{j\beta,i\alpha}, \tag{19}$$

where $\chi_{0l,m0}^k$ are response functions that depend on the d-band occupancy N_d, the electronic temperature T_e and the set of recursion coefficients $\{a_n^k, b_n^k\}$ associated with atom k. The $j\beta, i\alpha$ matrix elements of δa_m^k and δb_m^k are the interference terms that couple the orbitals $|j\beta\rangle$ and $|i\alpha\rangle$ together. They are given by

$$(\delta a_m^k)_{j\beta,i\alpha} = \sum_{r=1}^{2m+1} \frac{\partial a_m^k}{\partial \mu_r^k} (\zeta_{r+1})_{j\beta,i\alpha} \tag{20 a}$$

and

$$(\delta b_m^k)_{j\beta,i\alpha} = \sum_{r=1}^{2m} \frac{\partial b_m^k}{\partial \mu_r^k} (\zeta_{r+1})_{j\beta,i\alpha}. \tag{20 b}$$

where

$$(\zeta_{r+1})_{j\beta,i\alpha} = \langle j\beta | \hat{H}^r | i\alpha \rangle. \tag{20 c}$$

These interference terms are similar to the moments defined by equation (18) except that they link two sites rather than one.

Equation (19) therefore relates the bond order directly to the positions of the atoms locally through the many-body contributions that arise within the moment and interference term expansions. However, in practice, rather than summing over all the terms independently, it is computationally more efficient and numerically stable to use the method of O matrices. Here the reader is referred for further details to Horsfield *et al.* (1996a, Section IX). In addition, the infinite sum in equation (19) is truncated after several terms so that a truncator must be included in order to guarantee equivalence between the internal energy calculated via the on-site density-of-states through equation (12) and via the intersite density of states through equation (7) (Aoki 1993). The form of the truncator used is that given by equation (48) in the paper Bowler *et al.* (1997). We shall see in the next section that terms up to $m = 4$ are kept in equation (19) which corresponds to including nine exact moments of the density of states.

The tight-binding expression for the free energy, equation (2), contains no ionic contribution because the on-site energy levels E_i are adjusted self-consistently to maintain LCN. This is achieved efficiently within the BOP scheme by iterating the response functions. If the excess charge on site i is Q_i, then a good estimate of the shift that should be applied to the on-site energies to maintain LCN is

$$\Delta_i = -\frac{Q_i}{2\chi_{00.00}^i} \tag{21}$$

since $-2\chi_{00.00}^i = \partial N_d^i / \partial a_0^i$ and $a_0^i = E_i$. Using this prescription, usually no more than three or four iterations are needed to achieve convergence.

Finally, since the bond order is calculated in terms of the local environment, the computing time scales linearly with the number of atoms present in the simulation so that it is an order-N method†. At present the bond-order potential and the moments-based global density-of-states method (Horsfield 1996) are the only two viable order-N methods available for treating close-packed metals reliably (Bowler *et al.* 1997). However, atomistic calculations employing the bond-order potential can be expected to require about 10^2–10^3 times more computing time than similar calculations employing central-force many-body potentials and should therefore be employed only if the effect of non-central forces is essential for the problem studied.

§4. CONSTRUCTION OF A BOND ORDER POTENTIAL FOR TITANIUM

Since BOPs are not an *ab initio* method but follow the philosophy of parametrized tight-binding (Harrison 1980, 1994), both the bond (free) energy and the pairwise part of the energy are fitted so as to reproduce certain equilibrium properties of the material. The fitting of the bond part involves the bond integrals $dd\sigma(R)$, $dd\pi(R)$ and $dd\delta(R)$, the number N_d of valence d electrons and the electron temperature T_e, while fitting of the pairwise part involves the functional form of the potential $V(R)$. The equilibrium properties fitted are the electronic density of states, cohesive energy, equilibrium structure (i.e. lattice parameters a and c in the case of titanium) and elastic moduli. It is important to emphasize that the parameters entering the bond and pairwise parts were determined sequentially; first the bond integrals were established using a knowledge of the electronic structure and the Cauchy pressures, then the pair potential $V(R)$ was constructed to reproduce the remaining equilibrium properties of hcp Ti.

4.1. *Bond energy*

The tight-binding bond integrals are assumed to display a power-law dependence on distance, namely

$$dd\alpha(R) = dd\alpha_0 \left(\frac{R_0}{R}\right)^n \tag{22}$$

where $\alpha = \sigma$, π, or δ, $dd\alpha_0 = dd\alpha(R_0)$, and R_0 is the nearest-neighbour distance in the basal plane (2.950 Å for hcp Ti). The ratio of the three bond integrals is fixed by canonical band theory (Andersen 1975), namely $dd\sigma$: $dd\pi$:$dd\delta = -6$:4:-1. The magnitude of the integrals is chosen to give the correct width of the d band for Ti, 6.08 eV (Harrison 1980); this implies that $dd\sigma_0 = -0.689$ eV, $dd\pi_0 = 0.459$ eV and $dd\delta_0 = -0.115$ eV. Furthermore, in order to assure that the calculations remain within a reasonable computational time and memory requirements, a cut-off radius of 4.4 Å is introduced. This cut-off is smoothed by using a cubic spline for 3.1 Å $< R < 4.4$ Å instead of the power-law function given by equation (22). The coefficients in the cubic spline are chosen so that the polynomial and its first derivative are equal to the values given by equation (22) for $R = 3.1$ Å (just beyond the first-neighbour distance) and zero for $R = 4.4$ Å (just inside the third-nearest-neighbour distance). The functional form of the bond integrals is shown in figure 1.

---

† The computations were performed using the Oxford Order-N (OXON) package which is freely available on request: andrew.horsfield@materials.ox.ac.uk.
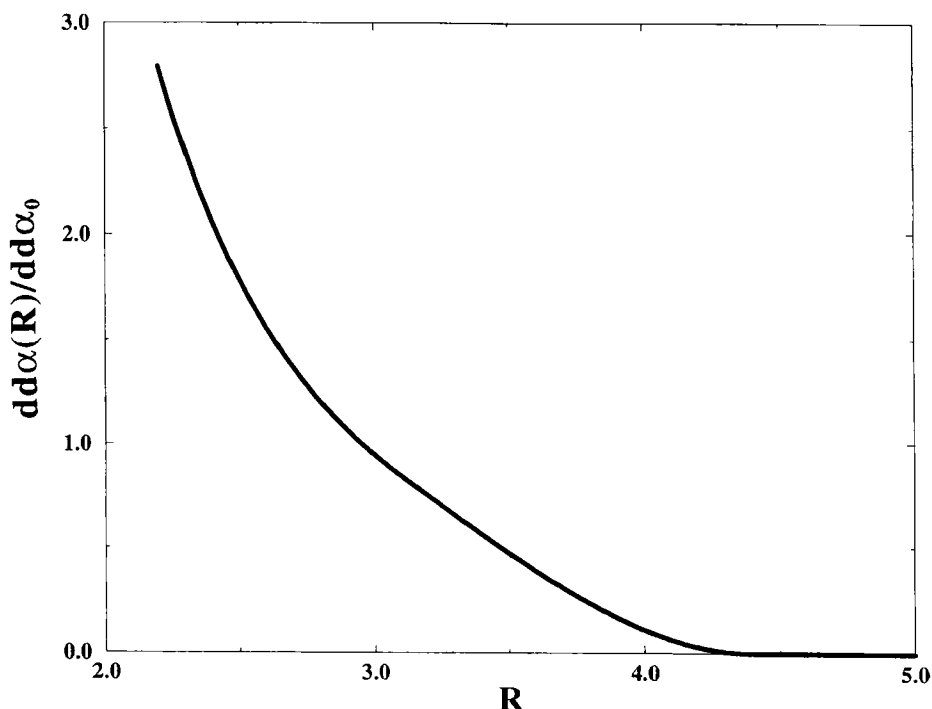
Figure 1.   Normalized bond integral $dd\alpha(R)/|dd\alpha_0|$ as a function of R (Å).

The number of exact recursion coefficients included in the bond-order potential expansion was chosen to ensure that the correct relative ordering of the energies of the hcp, fcc and bcc structures was obtained. The retention of the exact coefficients a_0, b_1 and a_1 up to the first level in the continued fraction in equation (14) is unable to distinguish between these three metallic structure types within a simple nearest neighbour tight-binding model (for example Pettifor (1995, p. 190)). The retention of exact coefficients up to the second level (i.e. including b_2 and a_2) leads to the bimodal distribution of the bcc density of states and the resultant stability of this lattice with respect to fcc and hcp for half-full bands (see Pettifor (1995, figure 8.20)). This was the motivation for the fourth-moment potentials developed for bcc transition metals by Carlsson (1991) and Moriarty (1994). However, the fourth-moment approxima-tion is unable to differentiate between the close-packed structures fcc and hcp. This requires including terms up to the third level in the continued fractions (i.e. including b_3 and a_3 or the sixth and seventh moments exactly). We have therefore taken our bond-order potential expansion to one further level beyond this minimum required for the prediction of cubic as against hcp stability or, equivalently, the value of the stacking-fault energy. Consequently, our potential has all moments exact up to and including the ninth. We have chosen a band filling of $N_d = 2$ which gives the correct relative ordering of fcc and bcc with respect to the ground-state hcp structure (see Pettifor (1995), figure 8.20).

As explained in §2 the effective electronic temperature T_e was introduced in order to dampen down the very long-range Friedel oscillations that can lead to slow con-vergence of the real-space bond-order expansions. We have chosen T_e sufficiently large to guarantee that the analytic Hellmann–Feynman force (equation (11)) and

Table 1. Forces acting on two atoms in the unit cell of the hcp lattice when atom 1 was displaced, calculated both analytically and numerically for $k_B T_e = 0.3\,\text{eV}$. The coordinate system is $x\|[\bar{1}\bar{1}20]$, $y\|[\bar{1}100]$ and $z\|[0001]$.

	Force (eV Å^{-1})		
	Analytic	Numerical	Difference
	Atom 1		
x component	−0.003 952	−0.003 946	0.000 006
y component	0.020 277	0.020 103	0.000 174
z component	0.001 465	0.002 002	0.000 537
	Atom 2		
x component	0.009 162	0.009 246	0.000 084
y component	−0.029 399	−0.029 042	0.000 357
z component	−0.030 168	−0.029 746	0.000 422

the force obtained by the *numerical* differentiation of the total energy (equation (1)), agreed to better than $0.0006\,\text{eV}\,\text{Å}^{-1}$. This has been attained for the value of $k_B T_e = 0.3\,\text{eV}$ which corresponds to $k_B T_e/W \approx \frac{1}{20}$, where W is the width of the d band. A comparison of analytic Hellman–Feynman forces with numerical differentiation of the total energy for two atoms within the unit cell of the hcp lattice is presented in table 1. In this calculation, one of the atoms in the unit cell was displaced away from its equilibrium position (atom 1) and the forces calculated on this and a neighbouring atom (2). This calculation illustrates that the analytic calculation agrees with the numerical calculation to the above precision.

The exponent n in equation (22) is chosen to give the best possible fit to the Cauchy pressures $C_{12} - C_{66}$ and $C_{13} - C_{44}$. As we have shown in the Appendix, these are independent of the pairwise part of the energy, being fully determined by the bond energy alone. Table 2 gives the dependence of these two Cauchy pressures on the exponent n. We have taken $n = 3.5$ for which the error in determination of both Cauchy pressures is very similar and which is close to the exponent expected for metals at the beginning of the transition series (see Pettifor (1995), table 7.1).

4.2. *Pairwise energy*

The functional form of the pair potential has been taken as

$$V(R) = \sum_{k=1}^{6} A_k (R_k - R)^3 H(R_k - R) + A \frac{(r_0 - R)^3}{R^{3.5}} H(r_0 - R), \qquad (23)$$

Table 2. Calculated Cauchy pressure for different values of the exponent n in equation (22). The experimental values are $C_{12} - C_{66} = 0.261\,\text{eV}\,\text{Å}^{-3}$ and $C_{13} - C_{44} = 0.109\,\text{eV}\,\text{Å}^{-3}$.

Exponent n	Calculated $C_{12} - C_{66}$ (eV Å^{-3})	Calculated $C_{13} - C_{44}$ (eV Å^{-3})
2.0	0.042	0.069
2.5	0.065	0.102
3.0	0.094	0.147
3.5	0.143	0.203
4.0	0.197	0.270
4.5	0.261	0.349

where $H(x)$ is the Heaviside step function. It is composed of two parts. The first part is a sum of cubic splines that extends up to the cut-off R_1, which lies in between the fourth and fifth neighbours in the ideal lattice. R_k are the node points of the splines and A_k numerical coefficients; both are used as fitting parameters as described below. This functional form assures that $V(R)$ and its first and second derivatives are everywhere continuous and equal to zero at the cut-off. Moreover, this form is very flexible since it allows for both the repulsive interaction at short separations of atoms and the attractive interaction at larger separations; the same form was used in construction of many-body central force potentials of the Finnis–Sinclair type (Ackland *et al.* 1987). The second part provides for a strongly repulsive core at atomic separations smaller than $r_0 = 2.80\,\text{Å}$, well below the nearest-neighbour spacing $(2.90\,\text{Å})$. This part was determined so as to follow closely the universal equation of state (Rose *et al.* 1983, 1984) for compressions up to 20%; this leads to $A = 100\,\text{eV}\,\text{Å}^{1/2}$. This part of the pair potential does not contribute to any of the equilibrium properties.

While keeping the bond part of the energy fixed, the parameters R_k and A_k of the pair potential have been determined by fitting the following quantities: the cohesive energy E_{coh}, two lattice parameters a and c and three of the five independent elastic moduli, namely C_{11}, C_{33} and C_{44}. The reason why all five elastic moduli have not been reproduced is that, in the case of the hexagonal symmetry, only three elastic moduli can be fitted independently since the Cauchy pressures $C_{12} - C_{66}$ and $C_{13} - C_{44}$ are fixed by the bond energy term (see the Appendix).

In the following relations which have been used in the fitting procedure, the superscripts p and b stand for pair potential contribution and bonding part contribution respectively; the quantities without superscripts are experimental (or *ab initio* calculated) values. Ω_0 is the volume of the unit cell and summation over i extends over all the atoms in the unit cell and summation over j over all the interacting neighbours of the atom i. The fitting of the cohesive energy leads to the equation

$$E_{\text{coh}}^{\text{p}} = \frac{1}{2\Omega_0} \sum_{i \neq j} V(R_{ij}) = E_{\text{coh}} - E_{\text{coh}}^{\text{b}}. \tag{24}$$

The equilibrium conditions determining the lattice parameters a and c can be formulated as the requirement that, in the coordinate system with the z axis parallel to the c axis of the hexagonal lattice, the stress components σ_{11} and σ_{33} vanish; the x axis is any direction perpendicular to the z axis. These conditions determine two other equations used in the fitting process (for more details see the Appendix)

$$\sigma_{11}^{\text{p}} = \frac{1}{2\Omega_0} \sum_i \sum_j V'(R_{ij}) \frac{X_{ij}^2}{R_{ij}} = -\sigma_{11}^{\text{b}}, \quad \sigma_{33}^{\text{p}} = \frac{1}{2\Omega_0} \sum_i \sum_j V'(R_{ij}) \frac{Z_{ij}^2}{R_{ij}} = -\sigma_{33}^{\text{b}}, \tag{25}$$

Finally, the relations for the elastic moduli determined for the equilibrium configuration lead to the additional three equations (for more details see the Appendix)

$$\frac{1}{2\Omega_0} \sum_i \sum_j \frac{\Psi(R_{ij})X_{ij}^4}{R_{ij}^2} = C_{11} - C_{11}^{\text{b}} + \sigma_{11}^{\text{b}}, \quad \frac{1}{2\Omega_0} \sum_i \sum_j \frac{\Psi(R_{ij})Z_{ij}^4}{R_{ij}^2} = C_{33} - C_{33}^{\text{b}} + \sigma_{33}^{\text{b}}$$

$$\frac{1}{2\Omega_0} \sum_i \sum_j \frac{\Psi(R_{ij})X_{ij}^2 Z_{ij}^2}{R_{ij}^2} = C_{44} - C_{44}^{\text{b}} + \tfrac{1}{4}(\sigma_{11}^{\text{b}} + \sigma_{33}^{\text{b}}), \tag{26}$$

Table 3. Experimental quantities fitted exactly.

E_{coh} (eV)	a (Å)	c/a	C_{11} (eV Å^{-3})	C_{33} (eV Å^{-3})	C_{44} (eV Å^{-3})
4.85	2.950	1.587	1.099	1.189	0.317

Table 4. Parameters of the pair potential.

k	A_k (eV Å^{-3})	R_k (Å)
1	$-0.323\,514\,535\,408\,23$	5.16
2	$0.301\,023\,144\,410\,33$	5.04
3	$0.379\,960\,532\,126\,67$	4.51
4	$-0.967\,269\,879\,486\,04$	4.12
5	$0.878\,210\,963\,253\,61$	3.93
6	$1.323\,928\,647\,346\,72$	3.25

where $\Psi(R) = V''(R) - V'(R)/R$. The quantities σ_{11}^b, σ_{33}^b, C_{11}^b, C_{33}^b and C_{44}^b have been evaluated numerically from the dependence of E_{coh}^b on the relevant applied strains. The experimental quantities which have been fitted exactly are summarized in table 3 and the parameters of the pair potential found by this fitting procedure are presented in table 4. The functional form of the pair potential is shown in figure 2.
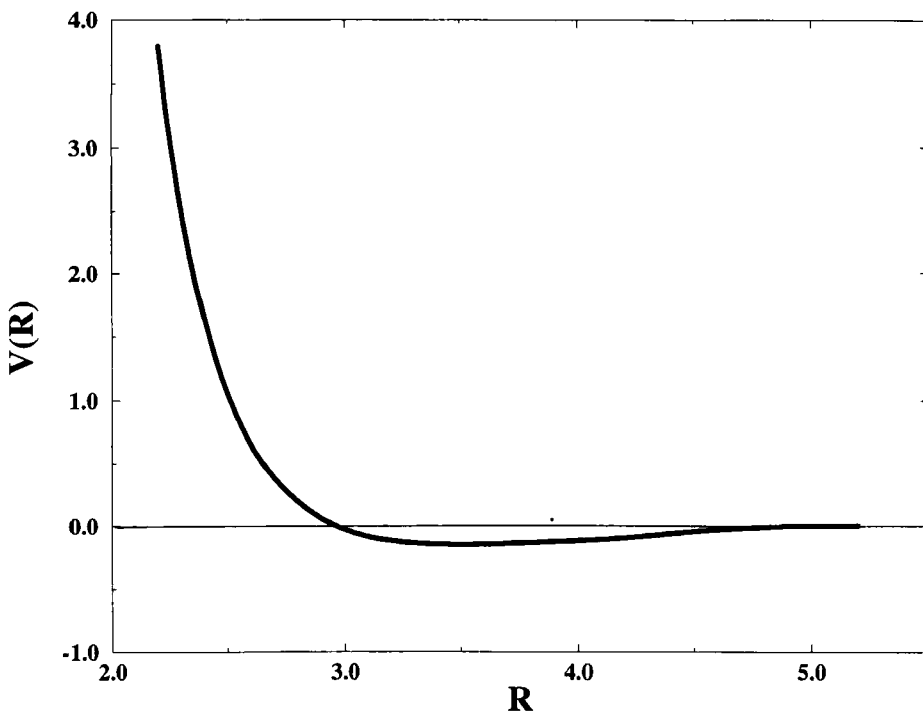
Figure 2. Pair potential V (eV) as a function of R (Å).

4.3. *Testing of the potential*

Since the reason for the development of the potential is its use in computer modelling of extended crystal defects, some unphysical structural instabilities or metastable configurations must not occur in the cores of such defects when using this potential. Whilst this can never be guaranteed absolutely, the following tests assure that such circumstances are unlikely to arise.

As explained above, not all the elastic constants have been fitted, and therefore the first test of the potential is to investigate how well the remaining moduli namely C_{12}, C_{13} and C_{66} (equal to $(C_{12} - C_{11})/2$), are reproduced. The calculated values of these elastic constants are $C_{12} = 0.462\,\text{eV}\,\text{Å}^{-3}$, $C_{13} = 0.520\,\text{eV}\,\text{Å}^{-3}$ and $C_{66} = 0.319\,\text{Å}^{-3}$ and the experimental values are $0.542\,\text{eV}\,\text{Å}^{-3}$, $0.426\,\text{eV}\,\text{Å}^{-3}$ and $0.281\,\text{eV}\,\text{Å}^{-3}$ respectively. It is seen that these elastic constants are reproduced to $\pm 0.1\,\text{eV}\,\text{Å}^{-3}$. The discrepancy is, of course, related to the precision with which the bond part reproduces the Cauchy pressures.

Since the elastic moduli are positively definite, the hcp structure is stable with respect to arbitrary small homogeneous deformations. However, when studying extended defects, large distortions of the local environment away from equilibrium are present. Hence, it is important that the ideal lattice structure is also stable with respect to large distortions. While this can never be fully examined, the most important tests are stability with respect to large shears parallel to some low-index crystal planes and stability with respect to large homogeneous strains. The former is effectively tested in calculations of γ surfaces (energy against displacement surfaces for
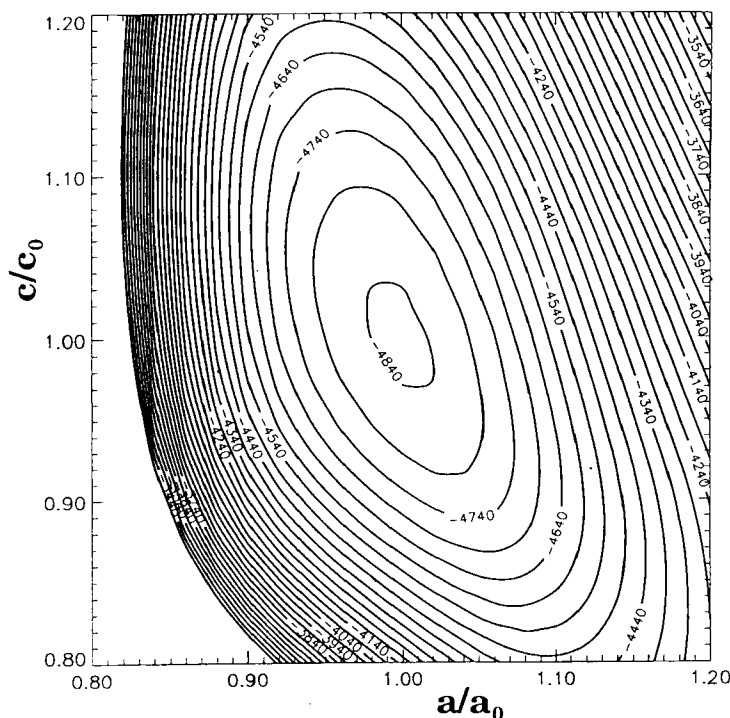

Figure 3.   Energy surface for large homogeneous deformations of the unit cell, where the values of the energies are in meV per atom.

certain crystallographic planes, for example Duesbery and Richardson (1991) and Vitek (1992)) which have been performed in the accompanying paper. Clearly, since the calculated γ surfaces for basal and prism planes display positive values of the energy for all displacements, the potential guarantees the mechanical stability of the hcp structure with respect to large shears in these planes. The latter has been tested by calculating the energy as a function of homogeneous expansions and contractions (by $\pm 20\%$) in the close-packed directions in the basal plane ($\langle 11\bar{2}0 \rangle$) and in the c direction ($\langle 0001 \rangle$) respectively. The results of this calculation are presented as the dependence of the energy on lattice parameters a and c in figure 3. The only minimum found on this energy surface corresponds to the fitted equilibrium values of the lattice parameters and thus no instabilities or metastable configurations occur for the range of deformations studied.

Another important condition which the potential must satisfy is that the fitted equilibrium structure is stable relative to alternate crystal structures with different symmetry, in particular those with a similar packing, such as fcc and bcc structures. This has been assured by the choice of the number N_d of valence d electrons. In both cases the cohesive energies are higher than for the hcp structure: in the fcc case by 0.030 eV per atom and in the bcc case by 0.074 eV per atom. The total energy calculations (Nguyen-Manh, *et al.* 1996) employing the full-potential linear muffin-tin orbitals method (Methfessel 1988) lead to somewhat larger differences of cohesive energies, namely 0.092 eV per atom and 0.128 eV per atom, for fcc and bcc structures respectively.

§5. CONCLUSIONS

The bond-order potential, presented in this paper, is eminently suitable for atomistic studies of crystal defects in hcp Ti; a study of screw dislocations employing this potential is presented in the part II. First, the potential reproduces exactly the equilibrium lattice parameters, in particular the non-ideal c/a ratio, and adequately the elastic moduli. Furthermore, it guarantees the stability of the hcp lattice with respect to most likely alternative structures, fcc and bcc, and mechanical stability with respect to large homogeneous expansions and contractions as well as with respect to large shears on basal and prism planes. Whilst these aspects of the description of atomic interactions can also be attained in the framework of central-force potentials (Ackland 1992), the bond-order potential reflects correctly the very important feature of cohesion in Ti, the directional covalent-type bonding arising due to the partially filled d band. This is achieved in the bond part by reproducing the canonical character of the d-band density of states, bandwidth and band filling favouring the hcp structure. Hence, this potential is likely to reveal correctly those structural features of lattice defects that are intimately related to the nature of bonding in Ti. However, quantitative calculations involving energy differences between similar structures may involve errors comparable with those encountered in a comparison of the energies of hcp, fcc and bcc structures.

APPENDIX

Equilibrium conditions and elastic moduli

In the following we assume that the energy (or free energy) E of a system of N particles is a known function of their positions, that is $E = E(\mathbf{R}_1, \mathbf{R}_2, \ldots, \mathbf{R}_N)$. Owing to the translational invariance, E depends only on the relative positions of the atoms forming the system, that is on the vectors $\mathbf{R}_{ij} = \mathbf{R}_i - \mathbf{R}_j$. We now consider that a small homogeneous strain tensor $\varepsilon_{\alpha\beta}$ has been applied to the system and each vector $\mathbf{R}_{ij}$ transforms initially such that

$$\mathbf{R}_{ij}^\alpha \to \mathbf{R}_{ij}^\alpha + \sum_{\beta=1}^{3} \varepsilon_{\alpha\beta} \mathbf{R}_{ij}^\beta. \tag{A 1}$$

This is the only change in atomic positions in centrosymmetric structures but, in general, additional internal relaxation of atomic positions may occur (Born and Huang 1954, Martin 1975a,b). In the hcp structures, which are not generally centrosymmetric, this additional relaxation is very small, in particular when the c/a ratio is close to ideal (Igarashi *et al.* 1991) and was not included in the present study.

Assuming the change in atomic positions given by equation (A 1) the change in energy is up to the second order in $\varepsilon_{\alpha\beta}$:

$$\Delta E = \sum_{\substack{i,k \\ k>i}} \sum_{\alpha,\beta=1}^{3} \frac{\partial E}{\partial R_{ik}^\alpha} R_{ik}^\beta \varepsilon_{\alpha\beta} + \frac{1}{2} \sum_{\substack{i,j,k,l \\ k>i,l>j}} \sum_{\alpha,\beta,\gamma,\delta=1}^{3} \frac{\partial^2 E}{\partial R_{ik}^\alpha \partial R_{jl}^\gamma} R_{ik}^\beta R_{jl}^\delta \varepsilon_{\alpha\beta} \varepsilon_{\gamma\delta}. \tag{A 2}$$

At the same time when considering the system as an elastic continuum the change in energy is

$$\Delta E = \Omega \left(\sum_{\alpha,\beta=1}^{3} \sigma_{\alpha\beta} \varepsilon_{\alpha\beta} + \frac{1}{2} \sum_{\alpha,\beta,\gamma,\delta=1}^{3} C_{\alpha\beta\gamma\delta} \varepsilon_{\alpha\beta} \varepsilon_{\gamma\delta} \right), \tag{A 3}$$

where Ω is the volume of the system, $\sigma_{\alpha\beta}$ the stress tensor and $C_{\alpha\beta\gamma\delta}$ the tensor of the second-order elastic moduli. Comparison of equations (A 2) and (A 3) yields

$$\sigma_{\alpha\beta} = \frac{1}{\Omega} \sum_{\substack{i,k \\ k>i}} \frac{\partial E}{\partial R_{ik}^\alpha} R_{ik}^\beta, \tag{A 4}$$

$$C_{\alpha\beta\gamma\delta} = \frac{1}{4\Omega} \sum_{\substack{i,j,k,l \\ k>i,l>j}} \left(\frac{\partial^2 E}{\partial R_{ik}^\alpha \partial R_{jl}^\gamma} R_{ik}^\beta R_{jl}^\delta + \frac{\partial^2 E}{\partial R_{ik}^\beta \partial R_{jl}^\gamma} R_{ik}^\alpha R_{jl}^\delta \right.$$
$$\left. + \frac{\partial^2 E}{\partial R_{ik}^\alpha \partial R_{jl}^\delta} R_{ik}^\beta R_{jl}^\gamma + \frac{\partial^2 E_{\text{tot}}}{\partial R_{ik}^\beta \partial_{jl}^\delta} R_{ik}^\alpha R_{jl}^\gamma \right). \tag{A 5}$$

When written in this form the elastic moduli automatically satisfy the required symmetry relations. The equilibrium conditions, arising from the requirement that in equilibrium the system is in a minimum-energy configuration with respect to any homogeneous applied strains, are $\sigma_{\alpha\beta} = 0$ and $C_{\alpha\beta\gamma\delta}$ is a positively defined matrix.

When the free energy of a system is given by equation (1) we can write

$$\sigma_{\alpha\beta} = \sigma_{\alpha\beta}^{\mathrm{p}} + \sigma_{\alpha\beta}^{\mathrm{b}}, \tag{A 6 a}$$

$$C_{\alpha\beta\gamma\delta} = C_{\alpha\beta\gamma\delta}^{\mathrm{p}} + C_{\alpha\beta\gamma\delta}^{\mathrm{b}}, \tag{A 6 b}$$

where the superscripts p and b denote contributions from the pairwise and bond part respectively, of the total free energy. The condition of equilibrium then is

$$\sigma_{\alpha\beta}^{\mathrm{p}} = -\sigma_{\alpha\beta}^{\mathrm{b}}. \tag{A 7}$$

On the basis of equations (A 4) and (A 5) we obtain

$$\sigma_{\alpha\beta}^{\mathrm{p}} = \frac{1}{2\Omega} \sum_{\substack{i,k \\ k \neq i}} \frac{\mathrm{d}V(R_{ik})}{\mathrm{d}R_{ik}} \frac{R_{ik}^{\alpha} R_{ik}^{\beta}}{R_{ik}}, \tag{A 8}$$

$$C_{\alpha\beta\gamma\delta}^{\mathrm{p}} = \frac{1}{2\Omega} \sum_{\substack{i,j \\ i \neq j}} \left(\frac{\Psi(R_{ij}) R_{ij}^{\alpha} R_{ij}^{\beta} R_{ij}^{\gamma} R_{ij}^{\delta}}{R_{ij}^2} \right.$$
$$\left. + \frac{1}{4R_{ij}} \frac{\mathrm{d}V(R_{ij})}{\mathrm{d}R_{ij}} (\delta_{\alpha\gamma} R_{ij}^{\beta} R_{ij}^{\delta} + \delta_{\beta\gamma} R_{ij}^{\alpha} R_{ij}^{\delta} + \delta_{\alpha\delta} R_{ij}^{\beta} R_{ij}^{\gamma} + \delta_{\beta\delta} R_{ij}^{\alpha} R_{ij}^{\gamma}) \right), \tag{A 9}$$

where

$$\Psi(R_{ij}) = \frac{\mathrm{d}^2 V(R_{ij})}{\mathrm{d}R_{ij}^2} - \frac{1}{R_{ij}} \frac{\mathrm{d}V(R_{ij})}{\mathrm{d}R_{ij}}.$$

Using equation (A 8) and the equilibrium condition (A 7) we can write

$$C_{\alpha\beta\gamma\delta}^{\mathrm{p}} = \frac{1}{2\Omega} \sum_{\substack{i,j \\ i \neq j}} \frac{\Psi(R_{ij}) R_{ij}^{\alpha} R_{ij}^{\beta} R_{ij}^{\gamma} R_{ij}^{\delta}}{R_{ij}^2} - \tfrac{1}{4}(\delta_{\alpha\gamma}\sigma_{\beta\gamma}^{\mathrm{b}} + \delta_{\beta\gamma}\sigma_{\alpha\delta}^{\mathrm{b}} + \delta_{\alpha\delta}\sigma_{\beta\gamma}^{\mathrm{b}} + \delta_{\beta\delta}\sigma_{\alpha\gamma}^{\mathrm{b}}) \tag{A 10}$$

In the following we shall use the usual non-tensorial notation for the elastic moduli which employs only two subscripts.

Let us consider the hexagonal symmetry with x_3 axis parallel to the sixfold c axis and x_1 and x_2 axes parallel to the twofold axes. In this case, $\sigma_{11} = \sigma_{22}$ and there are five independent elastic moduli C_{11}, C_{12}, C_{13}, C_{33}, C_{44}, $C_{66} = (C_{12} - C_{11})/2$. Following equation (A 10)

$$C_{11} = \frac{1}{2\Omega} \sum_{\substack{i,j \\ i \neq j}} \frac{\Psi(R_{ij})(R_{ij}^{(1)})^4}{R_{ij}^2} - \sigma_{11}^{b} + C_{11}^{b}, \tag{A 11 a}$$

$$C_{12} = \frac{1}{2\Omega} \sum_{\substack{i,j \\ i \neq j}} \frac{\Psi(R_{ij})(R_{ij}^{(1)})^2 (R_{ij}^{(2)})^2}{R_{ij}^2} + C_{12}^{b}, \tag{A 11 b}$$

$$C_{13} = \frac{1}{2\Omega} \sum_{\substack{i,j \\ i \neq j}} \frac{\Psi(R_{ij})(R_{ij}^{(1)})^2 (R_{ij}^{(3)})^2}{R_{ij}^2} + C_{13}^{b}, \tag{A 11 c}$$

$$C_{33} = \frac{1}{2\Omega} \sum_{\substack{i,j \\ i \neq j}} \frac{\Psi(R_{ij})(R_{ij}^{(3)})^4}{R_{ij}^2} - \sigma_{33}^{b} + C_{33}^{b}, \tag{A 11 d}$$

$$C_{44} = \frac{1}{2\Omega} \sum_{\substack{i,j \\ i \neq j}} \frac{\Psi(R_{ij})(R_{ij}^{(1)})^2 (R_{ij}^{(3)})^2}{R_{ij}^2} - \tfrac{1}{4}(\sigma_{11}^{b} + \sigma_{33}^{b}) + C_{44}^{b}, \tag{A 11 e}$$

$$C_{66} = \frac{1}{2\Omega} \sum_{\substack{i,j \\ i \neq j}} \frac{\Psi(R_{ij})(R_{ij}^{(1)})^2 (R_{ij}^{(2)})^2}{R_{ij}^2} - \tfrac{1}{2}\sigma_{11}^{b} + C_{66}^{b}. \tag{A 11 f}$$

The two Cauchy pressures are

$$C_{12} - C_{66} = C_{12}^{b} - C_{66}^{b} + \tfrac{1}{2}\sigma_{11}^{b} \tag{A 11 g}$$

and

$$C_{13} - C_{44} = C_{13}^{b} - C_{44}^{b} + \tfrac{1}{4}(\sigma_{11}^{b} + \sigma_{33}^{b}). \tag{A 11 h}$$

Obviously, they are both determined by the bond energy only. The same has been shown earlier for the case of the cubic symmetry by Sob and Vitek (1996).

REFERENCES

ACKLAND, G. J., 1992, *Phil. Mag.* A, **66**, 917.
ACKLAND, G. J., FINNIS, M. W., and VITEK, V., 1988, *J. Phys.* F, **18**, L153.
ACKLAND, G. J., and THETFORD, R., 1987, *Phil. Mag.* A. **56**, 15.
ACKLAND, G. J., TICHY, G., VITEK, V., and FINNIS, M. W., 1987, *Phil. Mag.* A, **56**, 735.
ANDERSEN, O. K., 1975, *Phys. Rev.* B, **12**, 3060.
AOKI, M., 1993, *Phys. Rev. Lett.,* **71**, 3842.
AOKI, M., and PETTIFOR, D. G., 1994, *Mater. Sci. Engng.,* A176, 19.
BEER, N., and PETTIFOR, D. G., 1984, *Structure and Phase Stability of Alloys,* edited by P. Phariseau and W. Temmerman (New York: Plenum).
BROUGHTON, J., BRISTOWE, P., and NEWSAM, J. (editors), 1993, *Materials Theory Modelling,* Materials Research Society Symposium Proceedings, Vol. 291 (Pittsburgh, Pennsylvania: Materials Research Society).
BORN, M., and HUANG, K., 1954, *Dynamical Theory of Crystal, Lattices* (Oxford: Clarendon), chapter 1.
BOWLER, D. R., AOKI, M., GORINGE, C. M., HORSEFIELD, A. P., and PETTIFOR, D. G., 1997, *Modelling Simul. Mater. Sci. Engng,* **5**, 199.
CARLSSON, A. E., 1991, *Phys. Rev.* B, **44**, 6590.
DAW, M. S., and BASKES, M. I., 1984, *Phys. Rev.* B, **29**, 6443.
DAW, M. S., FOILES, S. M., and BASKES, M. I., 1993, *Mater. Sci. Rep.* **9**, 251.
DUESBERY, M. S., and RICHARDSON, G. Y., 1991, *CRC Crit. Rev, Solid St. Mater. Sci.* **17**, 1.

FEYNMAN, R. P., 1939, *Phys. Rev.* **56**, 340.

FINNIS, M. W., and SINCLAIR, J. E., 1984, *Phil. Mag.* A, **50**, 45.

FOILES, S. M., 1993, *Phys. Rev.* B, **48**, 4287; 1996 *Mater. Res. Soc. Bull.*, **21**, 24.

FRIEDEL, J., 1969, *The Physics of Metals*, edited by J. M. Ziman (Cambridge University Press), p. 340.

GELATT, C. D., EHRENREICH, H., and WATSON, E., 1977, *Phys. Rev.* B, **15**, 1613.

GIRSHICK, A., PETTIFOR, D. G., and VITEK, V., 1998, *Phil. Mag.* A, **77**, 999.

GONIS, A., TURCHI, P. E. A., and KUDRNOVSKY, J. (editors) 1996, *Stability of Materials* NATO Advanced Study Institute Series (New York: Plenum).

HARRISON, W. A., 1980, *Electronic Structure and Properties of Solids* (San Francisco, California: Freeman); 1994, *Surf. Sci.,* **300**, 298.

HAYDOCK, R., 1980, *Solid St. Phys.,* **35**, 216.

HELLMANN, H., 1937, *Einführung in die Quantenchemie* (Leipzig: Deuticke).

HORSFIELD, A. P., 1996, *Mater. Sci. Engng.* **B37**, 219.

HORSFIELD, A. P., BRATKOVSKY, A. M., FEARN, M., PETTIFOR, D. G., and AOKI, M., 1996a, *Phys. Rev.* B, **53**, 12 694.

HORSFIELD, A. P., BRATKOVSKY, A. M., PETTIFOR, D. G., and AOKI, M., 1996b, *Phys. Rev.* B, **53**, 1656.

IGARASHI, M., KHANTHA, M., and VITEK, V., 1991, *Phil. Mag.* B, **63**, 603.

LANCZOS, C., 1950, *J. Res. natn. Bur. Stand.,* **45**, 225.

LUDWIG, M., and GUMBSCH, P., 1995, *Modelling Simul. Mater. Sci. Engng*, **3**, 533.

MARK, J. E., GLICKSMAN, M. E., and MARSH, S. P. (editors), 1992, *Computational Methods in Materials Science,* Materials Research Society Symposium Proceedings. Vol. 278 (Pittsburgh, Pennsylvania: Materials Research Society).

MARTIN, J. W., 1975a, *J. Phys.* C, **8**, 2837; 1975b, *ibid*, **8**, 2858.

MERMIN, N. D., 1965, *Phys. Rev.* A, **137**, 1441.

METHFESSEL, M., 1988, *Phys. Rev.* B, **38**, 1537.

MORIARTY, J. A., 1994, *Phys. Rev.* B, **49**, 12 431.

NGUYEN-MANH, D., PETTIFOR, D. G., SHAO, G., MIODOWNIK, A. P., and PASTUREL, A., 1996, *Phil. Mag.* A, **74**, 1385.

PETTIFOR, D. G., 1983, *Physical Metallurgy*, edited by R. W. Cahn and P. Haasen (Amsterdam: Elsevier), p. 147; 1989, *Phys. Rev. Lett.,* **63**, 2480; 1995, *Bonding and Structure of Molecules and Solids* (Oxford University Press).

PETTIFOR, D. G., AOKI, M., GUMBSCH, P, HORSFIELD, A. P., NGUYEN MANH, D., and VITEK, V., 1995, *Mater. Sci. Engng,* **A192–A193**, 24.

PETTIFOR, D. G., and COTTRELL, A. H. (editors) 1992, *Electron Theory in Alloy Design* (London: Institute of Materials).

PETTIFOR, D. G., SKINNER, A. J., and DAVIES, R. A., 1989, *Atomistic Simulations of Materials: Beyond, Pair Potentials,* edited by V. Vitek and D. Srolovitz (New York: Plenum), p. 317.

ROSE, J. H., SMITH, J. R., and FERRANTE, J., 1983, *Phys. Rev.* B, **28**, 1835.

ROSE, J. H., SMITH, J. R., GUINEA, F., and FERRANTE, J., 1984, *Phys. Rev.* B, **29**, 2963.

SKINNER, A. J., and PETTIFOR, D. G., 1991, *J. Phys.: condens. Matter,* **3**, 2029.

SLATER, J. C., and KOSTER, G. F., 1954, *Phys. Rev.,* **94**, 1498.

SOB, M., and VITEK, V., 1996, *Stability of Materials,* NATO Advanced Study Institute Series, edited by A. Gonis, P. E. A. Turchi and J. Kudrnovsky (New York: Plenum), p. 449.

SUTTON, A. P., FINNIS, M. W., PETTIFOR, D. G., and OHTA, Y., 1988, *J. Phys.* C, **21**, 35.

TERSOFF, J., VANDERBILT, D. and VITEK, V. (editors), 1989, *Atomic Scale Calculations in Materials Science,* Materials Research Society Symposium Proceedings, Vol. 141 (Pittsburgh, Pennsylvania: Materials Research Society).

VITEK, V., 1992, *Prog. Mater. Sci.,* **36**, 1; 1996, *Mater. Res Soc. Bull.,* **21**, 20.

VOTER, A. F., 1996, *Mater. Res. Soc. Bull.,* **21**, 17.

VOTER, A. F., and CHEN, S. P., 1987, *Characterization of Defects in Materials,* Materials Research Society Symposium Proceedings, Vol. 82, (edited by R. W. Siegel, R,. Sinclair and J. R. Weertman (Pittsburgh, Pennsylvania: Materials Research Society), p. 175.

XU, W., and MORIARTY, J. A., 1996, *Phys. Rev.* B, **54**, 6941.

YAN, M., VITEK, V., and CHEN, S. P., 1996, *Acta Mater.,* **44**, 4351.